This article has been accepted for publication in a future issue of this journal, but has not been fully edited. Content may change prior to final publication. Citation information: DOI 10.1109/LPT.2017.2723662, IEEE Photonics Technology Letters

Dual Polarization Discrete Changes Model of Inter-core Crosstalk in Multi-core Fibers

Ricardo O. J. Soeiro, Tiago M. F. Alves, and Adolfo V. T. Cartaxo

***Abstract*—The discrete changes model (DCM) of inter-core crosstalk (ICXT) in weakly-coupled homogeneous multi-core fibers (MCFs) is generalized to a dual polarization (DP) scheme. This model provides theoretical expressions for the two polarization fields of the ICXT at the MCF output. Therefore, it may be of particular interest in the design of direct-detection MCF systems where the photodetected ICXT results mainly from the beating between the ICXT field at the MCF output and the carrier of the interfered core. The DP-DCM is validated by comparison of the mean ICXT power and ICXT field amplitude estimates with the ones obtained with a rigorous, yet much more computationally demanding, model based on the coupled local mode theory (CLMT). Good agreement between the mean ICXT power estimates obtained with the DP-DCM and CLMT is observed when the inter-core coupling coefficient variation along the MCF is small. Good agreement is also observed when comparing the probability density functions of the ICXT field amplitude.**

***Index Terms*—multi-core fibers, crosstalk, discrete changes model, coupled local mode theory, dual polarization.**

I. Introduction

HOMOGENEOUS multi-core fibers (MCFs), whose cores have similar properties, have been reported as an attractive medium for signal transmission [1], [2]. However, homogeneous MCFs suffer from significant inter-core crosstalk (ICXT) [2]. The ICXT can be reduced by appropriate MCF design, e.g., by increasing the distance between cores, which has the disadvantage of reducing the core count, or by enveloping each core in a trench [1]. Such constraints fueled the proposal of several ICXT estimation models that take into account the parameters of the MCF. In [3], a discrete changes model (DCM), based on the coupled mode theory, was proposed to estimate the ICXT while assessing its dependence on the fiber bending, twist and length. The ICXT was reported to result mostly from the discrete contribution of phase matching points (PMPs), i.e. the points along the longitudinal propagation direction for which the difference between the effective refractive index of the interfering and interfered cores is zero [3]. In [2] and [4], the DCM was upgraded to include the dependence on the modulation frequency and difference between the dispersion parameters of the cores, respectively. The interest in upgrading the DCM to make it a more general model can be attributed to its computational efficiency when compared to models that rely on solving the coupled-mode equations numerically. In particular, the number of PMPs required to estimate the ICXT with the DCM is much smaller than the number of steps required to solve the coupled-mode equations numerically [5]. The models proposed in [3]-[5] for the ICXT field deal with a single polarization scheme. In [6], the ICXT is modeled by a rigorous coupled local mode theory (CLMT), accounting for the core birefringence. However, the CLMT estimates are much more computationally demanding when compared to the DCM, owing to the necessity of solving the CLMT equations numerically. In [7] and [8], the mean ICXT power is estimated from analytical expressions based on the average power coupling coefficients. This approach allows for quick mean ICXT power estimates but, unlike the models reported in [3]-[6], it does not allow to model the probability density functions (PDFs) of the time-varying ICXT field and analyze the correlation between the in-phase and quadrature components of the ICXT field.

In this paper, the DCM proposed in [5] is generalized to a dual polarization (DP) scheme, for weakly-coupled MCFs. This model enables obtaining the two polarization ICXT fields at the MCF output and is particularly interesting for the design of direct-detection MCF systems, in which the time-varying photodetected ICXT results mainly from the beating between the ICXT field component originated from the data signal of the interfering cores and the optical carrier field of the interfered core [9]. The DP-DCM is validated by comparing the mean ICXT power and PDFs of ICXT field with the ones obtained from the CLMT, which is much more computationally demanding.

II. DCM for a dual-polarization scheme

In this section, a DP-DCM of ICXT is proposed. In Fig. 1, a conceptual illustration of the DP-DCM is shown. Linear propagation along a weakly-coupled two-core MCF is considered, where m and n are the interfering and interfered cores, respectively. A linear combination of the field amplitudes in two perpendicular polarization directions, x and y, at the MCF input is considered. The slowly varying complex amplitude of the field at the input of core m, $A_m(z{=}0)$, where z is the longitudinal propagation direction, is distributed between the two directions x and y. The power distribution between the polarization directions is controlled by $\zeta{\in}\{0,1\}$ such that $A_{m,x}(0){=}\sqrt{\zeta}{\cdot}A_m(0)$ and $A_{m,y}(0){=}\sqrt{1-\zeta}{\cdot}A_m(0)$. $F_{x,x}$, $F_{x,y}$, $F_{y,x}$, $F_{y,y}$ are the functions that model the ICXT

This work was supported by Fundação para a Ciência e Tecnologia (FCT), Portugal, under the project AMEN-UID/EEA/50008/2013 of Instituto de Telecomunicações, and the FCT researcher contract IF/01225/2015/CP1310/CT0001.

R. O. J. Soeiro and T. M. F. Alves are with the Instituto de Telecomunicações, Lisboa 1049-001, Portugal (e-mail: outerelo.soeiro@gmail.com; tiago.alves@lx.it.pt).

A. V. T. Cartaxo is with ISCTE - Instituto Universitário de Lisboa, Lisboa 1649-026, Portugal. He is also with the Instituto de Telecomunicações, Lisboa 1049-001, Portugal (e-mail: adolfo.cartaxo@lx.it.pt).

This article has been accepted for publication in a future issue of this journal, but has not been fully edited. Content may change prior to final publication. Citation information: DOI 10.1109/LPT.2017.2723662, IEEE Photonics Technology Letters

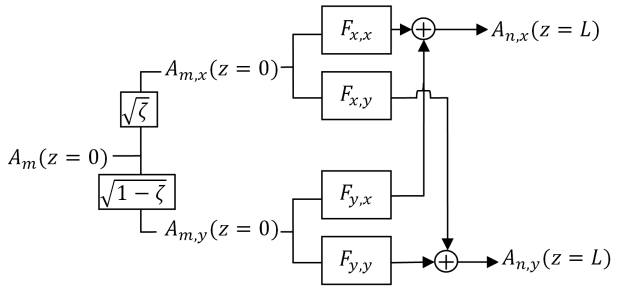

Fig. 1: Conceptual illustration of the DP-DCM.

from the input of core m to the output of core n, including the impact of the MCF parameters such as the fiber bending and twisting. In particular, $F_{x,x}$ and $F_{y,x}$ model the ICXT from polarizations x and y of core m to the polarization x of core n, respectively, and $F_{x,y}$ and $F_{y,y}$ model the ICXT from polarizations x and y of core m to the polarization y of core n, respectively. When no power is injected in core n, $A_{n,x}(L)$ and $A_{n,y}(L)$, with L the MCF length, are the ICXT fields of each polarization direction at the output of core n, which, from Fig. 1, are given by:

$$A_{n,x}(L) = A_m(0)\cdot[\sqrt{\zeta}\cdot F_{x,x} + \sqrt{1-\zeta}\cdot F_{y,x}] \quad (1)$$

$$A_{n,y}(L) = A_m(0)\cdot[\sqrt{1-\zeta}\cdot F_{y,y} + \sqrt{\zeta}\cdot F_{x,y}] \quad (2)$$

From Eqs. (1) and (2), the mean ICXT power of each polarization direction is given by:

$$\langle XT_x\rangle = \left\langle \frac{|A_{n,x}(L)|^2}{|A_m(0)|^2} \right\rangle = \zeta\cdot\langle|F_{x,x}|^2\rangle + (1-\zeta)\cdot\langle|F_{y,x}|^2\rangle + 2\Re\{\langle F_{x,x}\cdot F_{y,x}^*\rangle\cdot\sqrt{\zeta(1-\zeta)}\} \quad (3)$$

$$\langle XT_y\rangle = \left\langle \frac{|A_{n,y}(L)|^2}{|A_m(0)|^2} \right\rangle = \zeta\cdot\langle|F_{x,y}|^2\rangle + (1-\zeta)\cdot\langle|F_{y,y}|^2\rangle + 2\Re\{\langle F_{y,y}\cdot F_{x,y}^*\rangle\cdot\sqrt{\zeta(1-\zeta)}\} \quad (4)$$

where $\langle . \rangle$ is the expected value, $\Re\{.\}$ is the real part operator, and * is the complex conjugate operator.

Three conditions, used in this section to determine the functions F and validated in section III, are assumed: (i) due to random polarization mixing, the mean ICXT power of each polarization direction at the MCF output is the same ($\langle XT_x\rangle = \langle XT_y\rangle$), regardless the power distribution at the MCF input ($\forall\zeta\in[0,1]$); (ii) the mean ICXT power of core n, $\langle XT\rangle = \langle XT_x\rangle + \langle XT_y\rangle$, is the same $\forall\zeta\in[0,1]$; (iii) the in-phase and quadrature components of $A_{n,x}(L)$ and $A_{n,y}(L)$ are uncorrelated.

In the extreme case where all the power is injected in one of the polarizations at the MCF input ($\zeta = \{0,1\}$), Eqs. (3) and (4) can be written as:

$$\langle XT_x\rangle = \begin{cases} \langle|F_{x,x}|^2\rangle, & \zeta = 1 \\ \langle|F_{y,x}|^2\rangle, & \zeta = 0 \end{cases} \quad \langle XT_y\rangle = \begin{cases} \langle|F_{x,y}|^2\rangle, & \zeta = 1 \\ \langle|F_{y,y}|^2\rangle, & \zeta = 0 \end{cases} \quad (5)$$

From Eq. (5), the mean ICXT power of core n is:

$$\langle XT\rangle = \begin{cases} \langle|F_{x,x}|^2\rangle + \langle|F_{x,y}|^2\rangle, & \zeta = 1 \\ \langle|F_{y,y}|^2\rangle + \langle|F_{y,x}|^2\rangle, & \zeta = 0 \end{cases} \quad (6)$$

From the assumption that $\langle XT_x\rangle = \langle XT_y\rangle$, Eq. (5) yields $\langle|F_{x,x}|^2\rangle = \langle|F_{x,y}|^2\rangle$ and $\langle|F_{y,x}|^2\rangle = \langle|F_{y,y}|^2\rangle$. In addition, if $\langle XT\rangle$ is the same for $\zeta = \{0,1\}$, then from Eqs. (5) and (6) $\langle XT/2\rangle = \langle XT_x\rangle = \langle XT_y\rangle = \langle|F_{a,b}|^2\rangle$, $\forall a,b\in\{x,y\}$ and $\zeta = \{0,1\}$. The condition $\langle XT/2\rangle = \langle XT_x\rangle = \langle XT_y\rangle$ is valid for $\zeta\in[0,1]$ as long as $\langle F_{x,x}\cdot F_{y,x}^*\rangle = \langle F_{y,y}\cdot F_{x,y}^*\rangle = 0$, i.e. as long as $F_{x,x}$ and $F_{y,x}$, as well as $F_{y,y}$ and $F_{x,y}$, are uncorrelated, which, by substituting Eq. (5) on the left-hand side of Eqs. (3) and (4), yields $\langle XT/2\rangle = \langle XT_x\rangle = \langle XT_y\rangle = \langle|F_{a,b}|^2\rangle, \forall\zeta\in[0,1]$.

A complete description of the model entails also condition (iii). The ICXT polarization fields can be written as $A_{n,x} = A_{n,x,I} + jA_{n,x,Q}$ and $A_{n,y} = A_{n,y,I} + jA_{n,y,Q}$, where the MCF length is omitted for the sake of simplicity, and I and Q refer to the in-phase and quadrature components, respectively. The correlation between $A_{n,x}$ and $A_{n,y}$ is given by $\langle(A_{n,x,I} + jA_{n,x,Q})\cdot(A_{n,y,I} - jA_{n,y,Q})\rangle$. From Eqs. (1) and (2) it can also be expressed as $|A_m(0)|^2\cdot[\sqrt{\zeta}\sqrt{1-\zeta}(\langle F_{x,x}\cdot F_{y,y}^*\rangle + \langle F_{y,x}\cdot F_{x,y}^*\rangle) + \zeta\cdot\langle F_{x,x}\cdot F_{x,y}^*\rangle + (1-\zeta)\cdot\langle F_{y,x}\cdot F_{y,y}^*\rangle]$. Thus, one way to guarantee that the in-phase and quadrature components of $A_{n,x}$ and $A_{n,y}$ are uncorrelated regardless the value of ζ is to impose that the functions F shown above are uncorrelated, i.e. $\langle F_{x,x}\cdot F_{y,y}^*\rangle = \langle F_{y,x}\cdot F_{x,y}^*\rangle = \langle F_{x,x}\cdot F_{x,y}^*\rangle = \langle F_{y,x}\cdot F_{y,y}^*\rangle = 0$.

The functions F can be obtained from Eq. (33) of [5], for a single polarization DCM, and generalized to the DP-DCM scheme by considering that the impact of the terms referring to the polarization directions is averaged due to random polarization mixing:

$$F_{a,b} = \frac{-j}{\sqrt{2}}\cdot e^{-j\overline{\beta}_n L}\cdot\overline{K}'_{nm}\sum_{k=1}^{N} e^{-j(\overline{\beta}_m - \overline{\beta}_n)\cdot z_k} e^{-j\phi_{nm,k}^{(a,b)}} \quad (7)$$

where N is the number of PMPs, $\overline{K}'_{nm}$ is the discrete coupling coefficient obtained from Eq. (28) of [5] while substituting the inter-core coupling coefficient, κ_{nm}, by the average inter-core coupling coefficient of the polarizations, $\overline{\kappa}_{nm} = (\kappa_{nm}^{(x)} + \kappa_{nm}^{(y)})/2$. $\overline{\beta}_m$ and $\overline{\beta}_n$ are the average of the propagation constants of the polarizations in cores m and n, respectively, i.e., $\overline{\beta_m} = (\beta_m^{(x)} + \beta_m^{(y)})/2$ and $\overline{\beta_n} = (\beta_n^{(x)} + \beta_n^{(y)})/2$ [10]. $\phi_{nm,k}^{(a,b)}$ is a random variable, uniformly distributed between 0 and 2π, that models random variations of the fiber parameters [3]. The functions F are uncorrelated imposing that $\phi_{nm,k}^{(a_1,b_1)}$ and $\phi_{nm,k}^{(a_2,b_2)}$ are uncorrelated for $a_1 \neq a_2$ or $b_1 \neq b_2$. From Eq. (7) and Eq. (34) of [5], the mean ICXT power can be easily estimated from: $\langle XT\rangle = 2\langle XT_x\rangle = 2\langle XT_y\rangle = N|\overline{K}'_{nm}|^2$.

III. Numerical results and discussion

In this section, the model proposed in section II is validated through numerical simulation. In order to validate the DP-DCM, we start by validating the three conditions introduced in section II, which led to the conclusion that $\langle|F_{x,x}|^2\rangle = \langle|F_{y,x}|^2\rangle = \langle|F_{y,y}|^2\rangle = \langle|F_{x,y}|^2\rangle$. These conditions are validated using the rigorous CLMT model [6]. The coupling equations of the CLMT shown in [6] are solved numerically for linear propagation to estimate the longitudinal evolution of the slowly varying electric polarization field in each core. Each core is modeled as series of birefringent

This article has been accepted for publication in a future issue of this journal, but has not been fully edited. Content may change prior to final publication. Citation information: DOI 10.1109/LPT.2017.2723662, IEEE Photonics Technology Letters

segments where, at the beginning of each segment and MCF output, the rotation matrix shown in Eq. (2) of [11] is applied to the polarization fields of each core to guarantee random polarization coupling and, consequently, similar mean power distribution in the two polarization directions. Random temporal fluctuations and longitudinal fluctuations of the birefringence are considered as in [6]. In particular, the mean linear birefringence of each core is fixed between 10^{-7}, low birefringent (LB) core, and 10^{-4}, high birefringent (HB) core [6], and the birefringence standard deviation is 10^{-7}. The fiber twisting and bending is modeled by Eq. (19) of [6]. The inter-core coupling coefficient has a longitudinal fluctuation given by Eq. (12d) in [6]. The main parameters of the MCF considered in this study are shown in Table I. The number of segments considered for each core is 40 to guarantee a considerable amount of random birefringent segments along the fiber, and the mean ICXT power at the MCF output is estimated over 500 samples of MCF realizations. It was concluded that, with the parameters of Tab. I and perfectly homogeneous MCF, a larger number of segments or realizations leads to similar mean ICXT power estimates. For each realization, the birefringence of each segment is obtained from a Gaussian distribution [6].

TABLE I: 2-core MCF main parameters.

Parameter	Value
Core radius	4 μm
Refractive index of cladding	1.4381
Refractive index of core n (n_n)	variable
Refractive index of core m (n_m)	1.4453
Mean linear birefringence	variable
Linear birefringence standard deviation	10^{-7}
Distance between cores n and m (Λ_{nm})	30 μm
Bending radius	variable
Fiber twist frequency (f_T)	0.1 turns/m
Fiber length (L)	200 m
Wavelength	1550 nm

The mean ICXT power can be written in terms of the variance of the ICXT field amplitude of the I and Q components of the polarization directions, $\sigma^2_{m,i}$, where $m = \{x, y\}$ and $i = \{I, Q\}$, $\langle XT_x\rangle$=$\sigma^2_{x,I} + \sigma^2_{x,Q}$, and $\langle XT_y\rangle$=$\sigma^2_{y,I} + \sigma^2_{y,Q}$. Thus, $\langle XT\rangle$=$\sigma^2_{x,I}$+$\sigma^2_{x,Q}$+$\sigma^2_{y,I}$+$\sigma^2_{y,Q}$ [12]. Fig. 2 shows $\sigma^2_{m,i}$ for the two-core MCF and $\zeta = \{0, 0.5, 1\}$, as a function of the mean linear birefringence, for a bending radius of 0.2 m. From Fig. 2, it is concluded that the variance of the ICXT field amplitude is similar for all polarization directions, I and Q components, mean linear birefringence and ζ, with discrepancy not exceeding 1 dB. It follows from these results that conditions (i) and (ii), introduced in section II, are valid, showing consistency for a wide range of mean linear birefringence. Similar conclusions were drawn for a 4-core MCF with a central core interfered by three outer cores. The PDFs of the I and Q components of the ICXT field amplitude of the two polarization directions are shown in Fig. 2 as insets, for ζ=1 and mean linear birefringence of 2×10^{-7}. Those insets show that the PDFs of the I and Q components of the ICXT field amplitude of the two polarization directions are Gaussian distributed, as assumed in [7], [8], and that the DP-DCM provides estimates of the ICXT field amplitude in

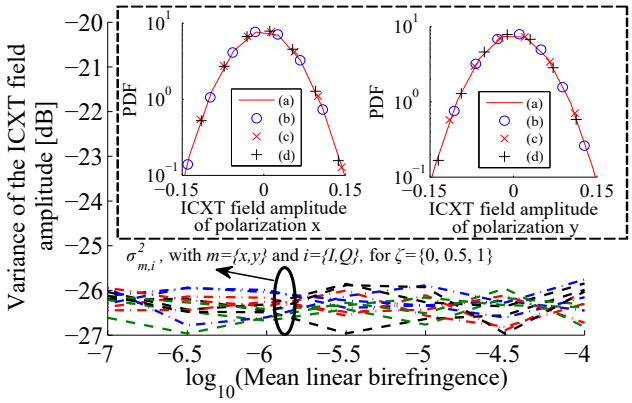

Fig. 2: Variance of the ICXT field amplitude, $\sigma^2_{m,i}$, as a function of the base-10 logarithm of the mean linear birefringence, obtained by the CLMT. The PDFs of the I and Q components of the ICXT field amplitude of the two polarization directions, obtained through simulation, are shown as insets for ζ=1 and mean linear birefringence of 2×10^{-7}. (a) I component (CLMT); (b) I component (DP-DCM); (c) Q component (CLMT); (d) Q component (DP-DCM).

good agreement with the CLMT. Similar conclusions were drawn for other bending radii, mean linear birefringences and ζ. It should be stressed that the DP-DCM proposed in this work allows evaluating the ICXT field amplitude of each polarization at the MCF output by using Eqs. (1), (2) and (7). In contrast, the analytical expressions reported in [7], [8] only allow to obtain the ICXT power. It was also observed that the in-phase and quadrature components of $A_{n,x}(L)$ and $A_{n,y}(L)$, obtained with the CLMT, are Gaussian distributed and uncorrelated, for different ζ, bending radii and mean linear birefringence. Thus, condition (iii) is validated.

Fig. 3 shows the mean ICXT power as a function of the bending radius, for a two-core perfectly homogeneous MCF ($n_n = n_m$). The results of Fig. 3 show that the mean ICXT powers obtained with the CLMT model for the LB and HB cases are similar, which agrees with the results of Fig. 2. More importantly, excellent agreement between the mean ICXT power estimates of the CLMT and DP-DCM is observed, with the discrepancy between the mean ICXT power estimates not exceeding 0.5 dB. This means that that the DP-DCM is applicable, in perfectly homogeneous MCFs, to a wide range of core birefringence and bending radii. Similar conclusions were also obtained for fiber twists of 0.01 and 0.05 turns/m.

Fig. 4 shows contours of the mean ICXT power, in decibel, for a two-core real homogeneous MCF [5], with $n_n = n_m(1+\Delta n^{(N)}_{nm})$. $\Delta n^{(N)}_{nm}$ is the normalized difference of refractive indexes between the cores n and m, i.e. $\Delta n^{(N)}_{nm} = (n_n - n_m)/n_m$. Very good agreement between the DP-DCM (see Fig. 4(a)) and the CLMT (see Fig. 4(b)) occurs also for real homogeneous MCFs, with the discrepancy between the mean ICXT power obtained with the models not exceeding 0.6 dB. This small discrepancy is achieved for small variations of κ_{nm} along the longitudinal direction of propagation, z, induced by fiber bending and twisting. Further investigation revealed that the discrepancy between the mean ICXT power estimates obtained from the DP-DCM and the CLMT can

This article has been accepted for publication in a future issue of this journal, but has not been fully edited. Content may change prior to final publication. Citation information: DOI 10.1109/LPT.2017.2723662, IEEE Photonics Technology Letters

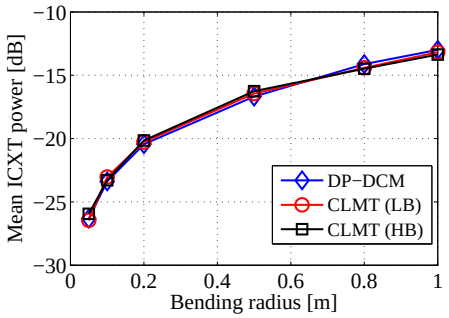

Fig. 3: Mean ICXT power as a function of the bending radius, for homogeneous MCFs. Two cases of mean linear birefringence, 2×10^{-7} (LB) and 10^{-4} (HB), are considered, and $\zeta = 1$.

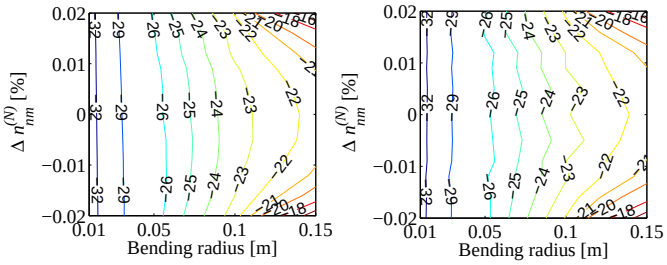

(a) Obtained with the DP-DCM. (b) Obtained with the CLMT.

Fig. 4: Contours of the mean ICXT power, in decibel, as a function of the normalized difference of refractive indexes between cores ($\Delta n_{nm}^{(N)}$), in percentage, and bending radius. A mean birefringence of 2×10^{-7} is considered and $\zeta = 1$.

increase to 3-4 dB when the variation of κ_{nm} along z is not negligible. In this case, the ICXT estimates of the DP-DCM are not accurate and generalization of the model to take into account the dependence of κ_{nm} on z is required. This study is left for future work. It should be noted that the bending radii shown in Figs. 4(a) and 4(b) are smaller than the ones of Fig. 3 because the critical bending radius, R_{th}, i.e. the maximum bending radius for which the DCM is valid, is smaller for larger $|\Delta n_{nm}^{(N)}|$, as $R_{th} = \Lambda_{nm}/|\Delta n_{nm}^{(N)}|$ [3], [5]. Thus, we have $R_{th} = 0.15$ m, for $|\Delta n_{nm}^{(N)}| = 0.02\%$ and $\Lambda_{nm} = 30$ μm. It was concluded that, if a 4-core MCF with 3 interfering cores with small κ_{nm} variations along z and $R_{th} = 0.25$ m is considered, the discrepancy of mean ICXT power estimates obtained with the CLMT and DP-DCM do not exceed 1 dB for bending radii not exceeding 0.21 m. For bending radii closer to R_{th}, the discrepancy may exceed 1 dB.

The results obtained with the CLMT model required solving numerically a system of differential equations with a small step. A maximum step of 10^{-4} m was considered in this paper, although it can be of the order of the wavelength if larger twisting rates are considered. In general, the number of steps is given by $L/\Delta z$, where Δz is the step size. In comparison, the number of PMPs used in the DP-DCM, given by $2f_T L$, is much smaller. For example, with $\Delta z = 10^{-4}$ m, $f_T = 0.1$ turns/m and $L = 200$ m, 2×10^7 steps are required. The mean ICXT power estimates obtained with such a large number of steps may take several days to obtain. In contrast, only 40 PMPs are used in the DP-DCM, under the same conditions, which allows for very fast estimates. Thus, the DP-DCM is much less computationally demanding, allowing for quick ICXT estimates without compromising accuracy.

IV. Conclusion

The DCM for ICXT estimation in weakly-coupled MCFs was generalized to a DP scheme and validated by comparison of the mean ICXT power and PDFs of the ICXT field amplitude estimates with the ones obtained with a more rigorous, yet much more computationally demanding, model based on the CLMT. Good agreement between the estimates of the mean ICXT power and of the PDFs of the ICXT field amplitude components of the polarization directions obtained from the DP-DCM and from the CLMT is observed for a small inter-core coupling coefficient variation along the MCF. The DP-DCM may be of particular interest for the performance analysis of MCF transmission systems employing direct-detection receivers, in which the time-varying photodetected ICXT results mainly from the beating between the ICXT field component of the interfering cores and the optical carrier field of the interfered core.

References

[1] J. Sakaguchi, B. Puttnam, W. Klaus, Y. Awaji, N. Wada, A. Kanno, T. Kawanishi, K. Imamura, H. Inaba, K. Mukasa, R. Sugizaki, T. Kobayashi, and M. Watanabe, "305 Tb/s space division multiplexed transmission using homogeneous 19-core fiber," *J. Lightw. Technol.*, vol. 31, no. 4, pp. 554-562, Feb. 2013.

[2] R. Luís, B. Puttnam , A. Cartaxo, W. Klaus, J. Mendinueta, Y. Awaji, N. Wada, T. Nakanishi, T. Hayashi, and T. Sasaki , "Time and modulation frequency dependence of crosstalk in homogeneous multi-core fibers," *J. Lightw. Technol.*, vol. 34, no. 2, pp. 441-447, Jan. 2016.

[3] T. Hayashi, T. Taru, O. Shimakawa, T. Sasaki, and E. Sasaoka, "Design and fabrication of ultra-low crosstalk and low-loss multi-core fiber," *Opt. Express*, vol. 19, no. 17, pp. 16576-16592, 2011.

[4] A. Cartaxo, R. Luís, B. Puttnam, T. Hayashi, Y. Awaji, and N. Wada, "Dispersion impact on the crosstalk amplitude response of homogeneous multi-core fibers," *Photon. Technol. Lett.*, vol. 28, no. 17, pp. 1858-1861, Sep. 2016.

[5] A. Cartaxo and T. Alves, "Discrete changes model of inter-core crosstalk of real homogeneous multi-core fibers," *J. Lightw. Technol.*, vol. 35, no. 12, pp. 2398-2408, Jun. 2017.

[6] A. Macho, C. García-Meca, F. Fraile-Peláez, M. Morant, and R. Llorente, "Birefringence effects in multi-core fiber: coupled local-mode theory," *Opt. Express*, vol. 24, no. 19, pp. 21415-21434, Sep. 2016.

[7] M. Koshiba, K. Saitoh, K. Takenaga, and S. Matsuo, "Analytical expression of average power-coupling coefficients for estimating intercore crosstalk in multicore fibers," *Photonics Journal*, vol. 4, no. 5, pp. 1987-1995, Sept. 2012.

[8] T. Hayashi, T. Sasaki, E. Sasaoka, K. Saitoh, and M. Koshiba, "Physical interpretation of intercore crosstalk in multicore fiber: effects of macrobend, structure fluctuation, and microbend," *Opt. Express*, vol. 21, no. 5, pp. 5401-5412, Mar. 2013.

[9] T. Alves, R. Luís, B. Puttnam, A. Cartaxo, Y. Awaji, and N. Wada, "Performance of adaptive DD-OFDM multicore fiber links and its relation with intercore crosstalk," *Opt. Express*, accepted for publication, 2017.

[10] G. Agrawal, "Nonlinear fiber optics," third edition, Academic Press, chapter 6, pp. 239-240.

[11] P. Wai, C. Menyuk, and H. Chen, "Stability of solitons in randomly varying birefringent fibers," *Opt. Lett.*, vol. 16, no. 16, pp. 1231-1233, 1991.

[12] T. Hayashi, T. Taru, O. Shimakawa, T. Sasaki, and E. Sasaoka "Characterization of crosstalk in ultra-low-crosstalk multi-core fiber," *J. Lightw. Technol.*, vol. 30, no. 4, Feb. 2012.